Self-Similarities in the Frequency-Amplitude Space of a Loss-Modulated CO_2 Laser

Cristian Bonatto,[1] Jean Claude Garreau,[2] and Jason A. C. Gallas[1,2]

[1]*Instituto de Física, Universidade Federal do Rio Grande do Sul, 91501-970 Porto Alegre, Brazil*

[2]*Laboratoire de Physique des Lasers, Atomes et Molécules, Centre d'Études et de Recherches Laser et Applications, Université des Sciences et Technologies de Lille, F-59655 Villeneuve d'Ascq cedex, France*

(Received 30 May 2005; published 29 September 2005)

We show the standard two-level continuous-time model of loss-modulated CO_2 lasers to display the same regular network of self-similar stability islands known so far to be typically present only in discrete-time models based on mappings. Our results suggest that the two-parameter space of class *B* laser models and that of a certain class of discrete mappings could be isomorphic.

DOI: 10.1103/PhysRevLett.95.143905 PACS numbers: 42.65.Sf, 05.45.Pq, 42.55.Ah

Lasers with modulated parameters are arguably among the simplest and most accessible laser systems of interest for applications in science and engineering and for theoretical investigations. The intrinsic interest in practical applications and in the nonlinear dynamics of modulated lasers has spurred a wide range of studies after the remarkably influential work of Arecchi *et al.* [1] reporting the first measurement of subharmonic bifurcations, multistability, and chaotic behavior in a *Q*-switched CO_2 laser. Since then, CO_2 lasers have been fruitfully exploited in many situations. Recent applications include studies of stochastic bifurcations in modulated CO_2 lasers [2], multistability induced by periodic modulations [3], rich nonlinear response of CO_2 lasers with current modulation and cavity detuning [4], and self-focusing effects in nematic liquid crystals [5].

In the last 20 years the CO_2 laser was extensively studied theoretically, numerically, and experimentally [6–8], but focusing mainly on the characterization of dynamical behaviors in phase space for specific parameters. For many systems, much more attention has been devoted to the description of phase-space dynamics than to the parameter space [6,9–11]. Concerning the parameter space of the CO_2 laser, Goswami [12] investigated analytically the first few period-doubling bifurcations for the Toda model of the laser [13].

The present Letter reports an investigation of the parameter space of a paradigmatic model of class *B* lasers, the CO_2 laser. More specifically, we study a popular two-level model of a CO_2 laser with modulated losses, focusing on the global stability of the laser with respect to the modulation, not the intensity. The remarkable discovery reported here is that stability islands of the *continuous*-time laser model emerge organized in a very regular network of self-similar structures called shrimps [14], illustrated in Figs. 1 and 2, and previously known to exist only in the parameter space of *discrete*-time dynamical systems [14–17]. Although there are theoretical grounds to expect them to be present [17], thus far all attempts to uncover shrimps in flows, i.e., in continuous-time dynamical systems modeled with sets of differential equations, have failed to produce them [18].

The single-mode dynamics of the loss-modulated CO_2 laser involves two coupled degrees of freedom and a time-dependent parameter which we write, as usual [3,6,7],

$$\frac{du}{dt} = \frac{1}{\tau}(z - k)u, \tag{1a}$$

$$\frac{dz}{dt} = (z_0 - z)\gamma - uz. \tag{1b}$$

Here, u is proportional to the radiation density, z and z_0 are the gain and unsaturated gain in the medium, respectively, τ denotes the transit time of the light in the laser cavity, γ is the gain decay rate, and $k \equiv k(t)$ represents the total cavity losses. The losses are modulated periodically as follows,

$$k(t) = k_0(1 + a\cos 2\pi f t), \tag{2}$$

where k_0 is the constant part of the losses and a and f, the amplitude and frequency of the modulation, are the main bifurcation parameters. The remaining parameters are fixed at $\tau = 3.5 \times 10^{-9}$ s, $\gamma = 1.978 \times 10^5$ s^{-1}, $z_0 = 0.175$, and $k_0 = 0.1731$, realistic values used in recent investigations [3]. Integrations were done using the standard fourth-order Runge-Kutta scheme with fixed time step, equal to $h = 4 \times 10^{-8}$. Phase diagrams in $a \times f$ space are obtained by computing Lyapunov exponents for a mesh of 600×600 equally spaced parameters. Starting from an arbitrary initial condition, we "followed the attractor", that is, after increasing parameters we initiated iterations using the last obtained values as the new initial conditions. The largest exponents were codified into a bit map with a continuous color scale ranging from the maximum positive (green) to maximum negative (blue) exponents. Zero exponents were codified in black. One of the exponents is always zero since it is simply related to the time evolution. Three illustrative bit maps for the laser model are shown in Fig. 1.

Figure 1(a) displays a global view of the parameter space. The most prominent features, the broad curved structures in Fig. 1(a), show that the parameter space of

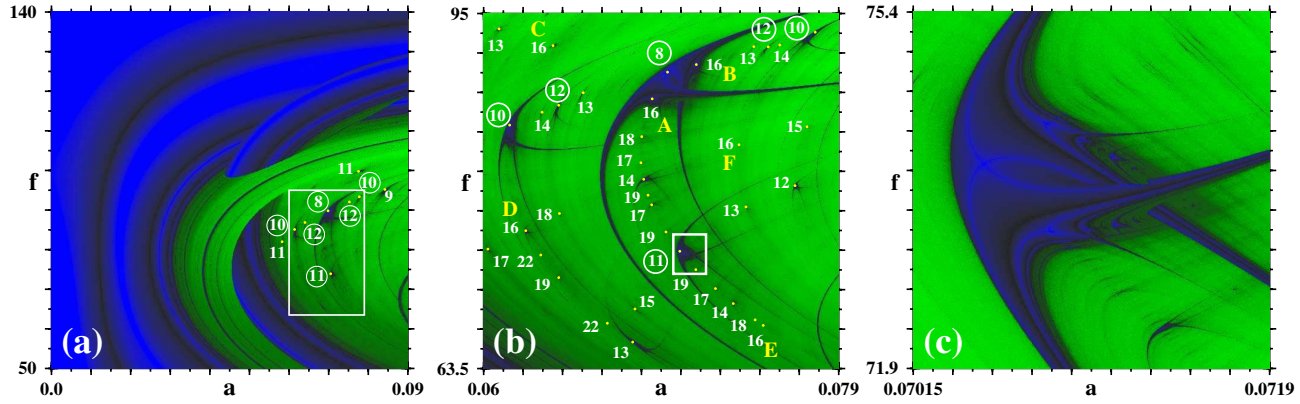

FIG. 1 (color online). Structure of the frequency-amplitude phase diagram of the laser showing a regular network of stability islands (a) Global view, (b) Zoom of the box in (a). Numbers indicate the main period of each stability island; (c) Magnification of the period-11 stability island [indicated in (b) by the encircled 11], displaying the generic shape of all stability islands [15]. Color intensities are proportional to Lyapunov exponents: blue (dark gray) for negative exponents (periodic oscillations), black for zero, and green (light gray) for positive exponents (chaotic oscillations). Frequencies are in kHz.

the laser model above, Eqs. (1a) and (1b), agrees qualitatively quite well with the description of Goswami [12] for the Toda model of the CO_2 laser. For the parameters chosen, the relaxation frequency of our laser model is 50 kHz. From Fig. 1(a) it is possible to see that there is a minimum amplitude threshold a beyond which subharmonic bifurcations start to occur, corresponding to about 100 kHz, the harmonic of the relaxation frequency. In addition, for certain parameter values new stability domains are created by saddle-node bifurcations, each of them undergoing then its own cascade of period doublings. So, in certain parameter ranges more than one stable mode coexist, giving rise to generalized multistability. This feature may be recognized in Fig. 1 from the apparent sudden discontinuities in the coloring, due only to the impossibility of plotting two distinct shades in the same place.

The most interesting feature in Fig. 1(a) is the remarkably regular structuring which appears in the region containing the box, shown magnified in Fig. 1(b). This figure shows that embedded in the wide domain of parameters leading to chaotic laser oscillations there is a regular structuring of self-similar parameter windows, shrimps, containing cascades of stable periodic oscillations, the *main period* of a few of the larger shrimps indicated by the number near to them. The period-11 shrimp seen in Fig. 1(b) is shown magnified in Fig. 1(c). Starting from the main period-11 body, it displays two distinct doubling cascades as well as an infinite number of additional period-doubling cascades, as thoroughly described for discrete-time systems in Refs. [14,15].

The computation of bit maps for the laser model is very computer demanding. To alleviate this problem and to manifest the isomorphism between the parameter spaces of flows and maps, we display the generic fine and hyperfine structure of stability islands typically present in multidimensional systems using the two-parameter Hénon map as a paradigm:

$$x_{t+1} = a - x_t^2 + by_t, \qquad y_{t+1} = x_t. \tag{3}$$

The nonlinearity parameter a (forcing) represents the bifurcation or control parameter. The damping parameter b varies between $-1 \leq b \leq 1$, with $b = 1$ representing the conservative limit and $b = 0$ the limit of strong damping. While for $b = 0$ there exists just a single attractor over a wide range of the parameter a, several periodic and chaotic attractors may coexist when $b \neq 0$.

We consider here the strongly dissipative limit, focusing on slightly negative values of b where Pando *et al.* [19] found that a sophisticated four-level model of the laser behaves qualitatively similar to the Hénon map. The CO_2 laser dynamics, as that of any class B laser, is characterized by a time delay between the intensity and the population inversion, a fact that nicely matches the delayed character of the Hénon map when written as a one-dimensional recurrence relation.

Figure 2 shows how regularly shrimps organize themselves along very *specific directions* in parameter space. The ordering along the main diagonal of Fig. 2(a) is the same found for the laser, in Fig. 1(a), along the direction containing the encircled periods. Analogously, the secondary diagonal in Fig. 2(a) displays the same ordering that the parabolic arc in the middle of Fig. 1(c).

The laser-Hénon agreement in parameter space permeates also to the phase space as corroborated by Fig. 3, comparing return maps for the laser (on the left column) with those for the Hénon map (right column). The laser return maps were constructed using the sequence $u_l(t)$, $l = 1, 2, 3, \ldots$ of normalized relative maxima of $u(t)$. As it is easy to see, both sets of return maps agree remarkably well [20].

How easy is it to detect experimentally the regular structuring reported here? Figure 4 illustrates a representative laser signal in two scales. Although waveforms and underlying periodicities are easy to recognize in logarith-

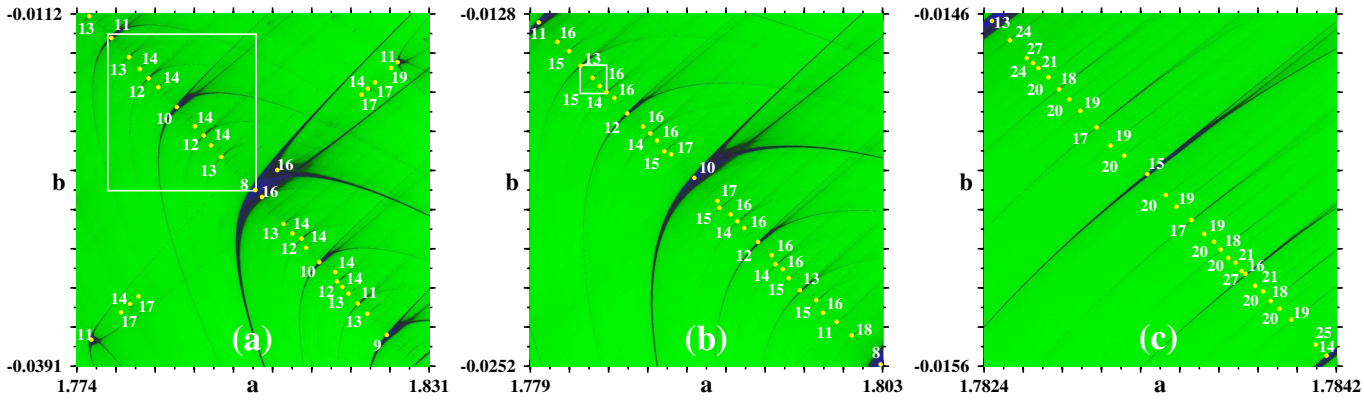

FIG. 2 (color online). Structure of the parameter space of the Hénon map. (a) The organization of shrimps here coincides with that of the laser [see Fig. 1(b)]. The fine structure observed around period-8 here reproduces the laser period-8 sequence along the curve passing by the encircled numbers in Fig. 1(b). (b) Magnification of the box in (a). (c) Magnification of the box in (b). Numbers indicate the main period of each stability island. Points mark windows, not doubly superstable crossings.

mic scale, their experimental detection may become strenuous, particularly as the period increases. For instance, contemplating the six period-16 stability islands in Fig. 1(b), two of them arising from period-8 via period-doubling bifurcations, one may ask what sort of differences should be expected in their measurement. The answer is depicted in Fig. 5. In a real experimental setup, the difficulties to surmount are mainly to access narrow high-period windows, and to have a wide enough detection range. Modulated losses are usually obtained with an intracavity polarizer and an electro-optical modulator. Recent progress in low-voltage electro-optical modulators have considerably improved their performances [21]. To detect large and small peaks simultaneously one can use a logarithmic preamplifier [22]. Thus, detection and discrimination of the laser signals in Fig. 5 is experimentally feasible with existing technology. We believe our investigation to shed new light on a matter which seemed already fully explored, opening new challenges for experimentalists and having potential applications beyond the selected example.

To uncover isomorphisms between the parameter space of continuous-time (flows) and discrete-time (maps) is an important event both from a physical and a dynamical point of view. In this context, we emphasize a relevant result of Hunt *et al.* [17] showing that for two-parameter systems there is a canonical family of quartic maps such that, typically, the bifurcations within a periodic window of a given scalar map are well approximated by a linear transformation of the bifurcation diagram of the canonical quartic map. For practical applications, an important question now is to investigate if parameter isomorphisms

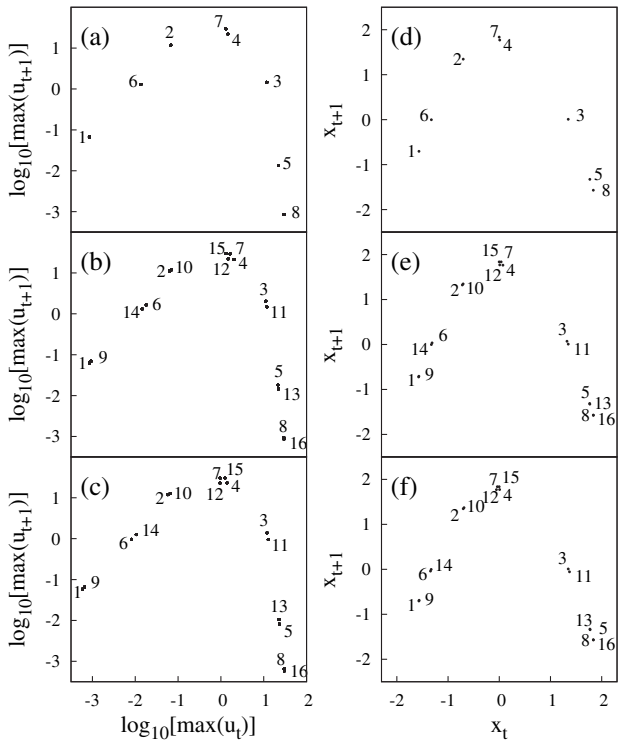

FIG. 3. Comparison of return maps. Left column: Laser return maps for period-8 and its pair of doublings. Parameters are: (a) $(a, f) = (0.06\,984, 89.8)$, period 8, (b) $(0.07\,138,\ 90.47)$, period-16, (c) $(0.06\,902,\ 87.43)$, period-16. Frequencies are in kHz. Right column: Hénon return maps for period-8 and its doublings seen at the center of Fig. 2(a). Parameters are: (d) $(a, b) = (1.80\,287, -0.02\,514)$, period-8, (e) $(1.80\,395, -0.0257)$, period-16, (f) $(1.80\,642, -0.02\,356)$, period-16.

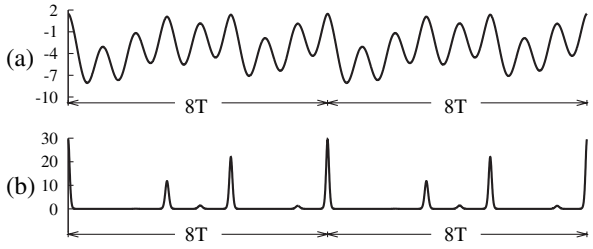

FIG. 4. Time evolution of the laser intensity $u(t)$ for the large period-8 structure in Fig. 1(b), plotted in (a) logarithmic scale, (b) linear scale. Here $T = 1/(89.8\ \text{kHz})$ is the period of the modulation.

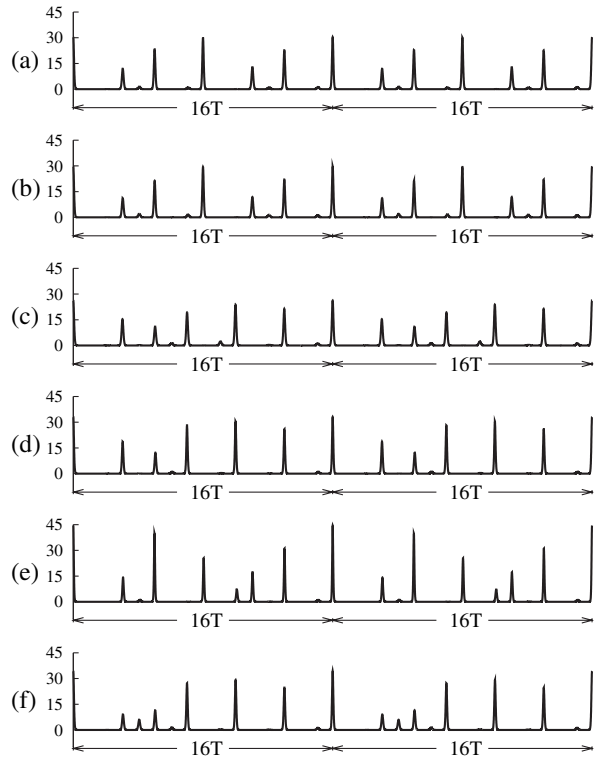

FIG. 5. Predicted signal intensity for the six period-16 stability islands labeled $A, B, \ldots F$, in Fig. 1(b). Signals (a) and (b), at points A and B, are period-8 doublings. All other signals are from islands which begin with period-16. Note that signals look very similar, despite the fact that they originate from very distinct regions of the parameter space. Parameters (a, f) are: (a) $A = (0.06\,902, 87.43)$, (b) $B = (0.07\,138, 90.47)$, (c) $C = (0.063\,725, 92.15)$, (d) $D = (0.062\,255, 75.735)$, (e) $E = (0.0\,749\,617, 67.3281)$, (f) $F = (0.073\,666, 83.359)$. Note that $T \equiv 1/f$ is slightly different for each signal.

should be expected also for more refined laser models such as those discussed in Refs. [23–25]. For these systems it would be useful to know what sort of basin entanglements exist for multistable domains where self-similar structures are abundant [26]. To conclude, let us briefly mention preliminary results showing that shrimps also exist for systems of autonomous differential equations as well as in semiconductor lasers subjected to optical injection. This will be reported elsewhere.

We thank Pierre Glorieux for a critical reading of the manuscript and helpful suggestions. C. B. thanks Conselho Nacional de Desenvolvimento Científico e Tecnológico (CNPq), Brazil, for support. J. A. C. G. thanks CNPq and the Université de Lille for support.

[1] F. T. Arecchi, R. Meucci, G. Puccioni, and J. Tredicce, Phys. Rev. Lett. **49**, 1217 (1982).

[2] L. Billings, I. B. Schwartz, D. S. Morgan, E. M. Bollt, R. Meucci, and E. Allaria, Phys. Rev. E **70**, 026220 (2004).

[3] V. N. Chizhevsky, Phys. Rev. E **64**, 036223 (2001).

[4] A. N. Pisarchik and B. F. Kuntsevich, J. Opt. B **3**, 363 (2001).

[5] S. Brugioni and R. Meucci, Eur. Phys. J. D **28**, 277 (2004).

[6] R. Gilmore and M. Lefranc, *The Topology of Chaos, Alice in Stretch and Squeezeland* (Wiley, New York, 2002); R. Gilmore, Rev. Mod. Phys. **70**, 1455 (1998).

[7] J. R. Tredicce, F. T. Arecchi, G. P. Puccioni, A. Poggi, and W. Gadomski, Phys. Rev. A **34**, 2073 (1986).

[8] D. Dangoisse, P. Glorieux, and D. Hennequin, Phys. Rev. A **36**, 4775 (1987); Phys. Rev. Lett. **57**, 2657 (1986).

[9] E. Ott, *Chaos in Dynamical Systems* (Cambridge University Press, Cambridge, England, 2002), 2nd ed.; K. T. Alligood, T. D. Sauer, and J. A. Yorke, *Chaos: An Introduction to Dynamical Systems* (Springer, New York, 1997).

[10] R. C. Hilborn, *Chaos and Nonlinear Dynamics: An Introduction for Scientists and Engineers* (Oxford University, Oxford, 2000), 2nd ed.

[11] S. H. Strogatz, *Nonlinear Dynamics and Chaos* (Perseus, Cambridge MA, 1994).

[12] B. K. Goswami, Phys. Lett. A **245**, 97 (1998).

[13] G. L. Oppo and A. Politi, Z. Phys. B **59**, 111 (1985).

[14] J. A. C. Gallas, Phys. Rev. Lett. **70**, 2714 (1993); Physica A (Amsterdam) **202**, 196 (1994).

[15] J. A. C. Gallas, Appl. Phys. B **60**, S-203 (1995), special supplement, Festschrift Herbert Walther.

[16] J. A. C. Gallas and H. E. Nusse, J. Econ. Behav. Organ. **29**, 447 (1996).

[17] B. R. Hunt, J. A. C. Gallas, C. Grebogi, J. A. Yorke, and H. Koçak, Physica D (Amsterdam) **129**, 35 (1999).

[18] M. Thiel, M. C. Romano, W. von Bloh, and J. Kurths kindly informed us to have recently found *shrimps* while computing recurrence plots.

[19] C. L. Pando, G. A. Luna Acosta, R. Meucci, and M. Ciofini, Phys. Lett. A **199**, 191 (1995).

[20] A prototypical map particularly suited to investigate analytically the inner structure of stability islands is the *canonical* quartic map $x_{t+1} = (x_t^2 - a)^2 - b$, introduced in Ref. [14] and discussed at length in Refs. [15,17].

[21] V. Berger, N. Vodjdani, D. Delacourt, and J. P. Schnell, Appl. Phys. Lett. **68**, 1904 (1996).

[22] M. Lefranc, D. Hennequin, and P. Glorieux, Phys. Lett. A **163**, 269 (1992).

[23] M. Ciofini, A. Politi, and R. Meucci, Phys. Rev. A **48**, 605 (1993).

[24] C. L. Pando, R. Meucci, M. Ciofini, and F. T. Arecchi, Chaos **3**, 279 (1993).

[25] R. Meucci, D. Cinotti, E. Allaria, L. Billings, I. Triandaf, D. Morgan, and I. B. Schwartz, Physica D (Amsterdam) **189**, 70 (2004).

[26] P. C. Rech, M. W. Beims, and J. A. C. Gallas, Phys. Rev. E **71**, 017202 (2005).